On the energy dependence of the D^+/D^- production asymmetry

E.R. Cazaroto[1], V.P. Goncalves[2], F.S. Navarra[1] and M. Nielsen[1]
[1] *Instituto de Física, Universidade de São Paulo, C.P. 66318, CEP 05315-970, São Paulo, SP, Brazil*
[2] *Instituto de Física e Matemática, Universidade Federal de Pelotas C. P. 354, CEP 96010-900, Pelotas, RS, Brazil*

In this paper we discuss the origin of the asymmetry present in D meson production and its energy dependence. In particular, we have applied the meson cloud model to calculate the asymmetries in D^-/D^+ meson production in high energy $p-p$ collisions and find a good agreement with recent LHCb data. Although small, this non-vanishing asymmetry may shed light on the role played by the charm meson cloud of the proton.

PACS numbers: 12.38.-t, 12.38.Bx, 13.60.Le

I. INTRODUCTION

It is experimentally well known [1–6] that there is a significant difference between the x_F (Feynman momentum) distributions of D^+ and D^- mesons produced in hadronic collisions with proton, Σ^- and pion projectiles. It is usually quantified in terms of the asymmetry function:

$$A = \frac{N_{D^-} - N_{D^+}}{N_{D^-} + N_{D^+}} \tag{1}$$

where N may represent the number of mesons of a specific type or its distribution in x_F, rapidity y and p_T. The recent data of the COMPASS collaboration [7] have confirmed the existence of charm production asymmetries also in γp collisions. Moreover, the very recent data from the LHCb collaboration [8] showed that there is asymmetry in the production of D^+ and D^- mesons in proton-proton collisions at 7 TeV. The origin of these asymmetries is still an open question. It is not possible to understand these production asymmetries only with usual perturbative QCD (pQCD) or with the string fragmentation model contained in PYTHIA. This has motivated the construction of alternative models [9–11] which were able to obtain a reasonable description of the low energy data and make concrete predictions for higher energy collisions. The LHCb data allow us, for the first time, to compare the predictions of the models with high energy data. Moreover, studying the energy dependence of production asymmetries, it may be possible to learn more about forward charm production, which undoubtedly has a non-perturbative component [10]. In this work we update one of these models, the meson cloud model or MCM [9], and compare its predictions with the new LHCb data.

Let us now briefly review some ideas about charm production. In perturbative QCD the most relevant elementary processes which are responsible for charm production are $q + \bar{q} \to c + \bar{c}$ and $g + g \to c + \bar{c}$. At high energies, due to the growth of the gluon distributions, the latter should be dominant. In standard pQCD, after being produced the c and $\bar{c}$ quarks fragment independently and hence, the resulting mesons D^+ and D^- (also D^0 and $\bar{D}^0$) will have the same rapidity, p_T and x_F distributions. This is indeed true for the bulk of charm production. Differences between the D^+ and D^- x_F distributions appear at large x_F, with D^- being harder. Given the valence quark content of the proton $p(uud)$ and of the $D^-(d\bar{c})$, a natural explanation of the observed effect is that the $\bar{c}$ is dragged by the projectile valence d quark, forming the, somewhat harder, $d\bar{c}$ bound state. This process has been usually called recombination or coalescence and it is illustrated in Fig. 1. This is a non-perturbative process and recombination models have been first proposed long time ago [12–14] and then used more recently [15, 16] to study the accumulated experimental data and to make predictions for the RHIC collisions. Unfortunately, the current RHIC experimental set up did not allow for a precise determination of production asymmetries. However, a more detailed analysis of the heavy quark sector is expected to be possible in the upgraded RHIC facility - RHIC II [17].

An alternative way to implement the idea of recombination is to use a purely hadronic picture of charm production, in which, instead of producing charm pairs and then recombining them with the valence quarks, we assume that the incoming proton fluctuates into a virtual charm meson - charm baryon pair, which may be liberated during the interaction with the target. This kind of fluctuation is unavoidable in any field theoretical description of hadrons and, in fact, it was shown [18] to be quite relevant to the understanding of hadron structure. It has been also successfully applied to particle production in high energy soft hadron collisions [19, 20] and in [9] it has been extended to the charm sector. This mechanism, in which the "meson cloud" plays a major role, is quite economical and can be improved systematically (see [21] for light mesons). From now on we shall call it meson cloud model (MCM). A simple and accurate description of charm asymmetry production at lower energies ($\sqrt{s} \simeq 10 - 40$ GeV) within the framework of the

MCM can be found in [22].

Another popular model of forward charm production is the intrinsic charm model (ICM) [10, 11, 23]. The existence of an intrinsic charm component in the wave function enhances charm meson production at large x_F. While IC, as formulated in [10, 11] is supported by several phenomenological analises, it is, alone, not enough to explain the difference between the D^+ and D^- x_F distributions. It is necessary to add a recombination mechanism (or "coalescence") in this kind of model to account for the observed asymmetries. In [10, 11] the intrinsic charm component of the proton is the higher Fock state $|uudc\bar{c}\rangle$ and its existence is attributed to a multigluon fusion, which is not calculable in pQCD. In [9] the intrinsic charm component of the proton was a consequence of the meson-baryon fluctuations mentioned above. In this approach, since they "feel" the virtual bound states where they once were, the c and $\bar{c}$ distributions are different from the beginning and when they later undergo independent fragmentation their difference will be transmitted to the final D mesons. Thus, in its "meson cloud" version, intrinsic charm may account for large x_F charm meson production including the asymmetries. The charm quarks of the projectile wave function traverse the target and fragment independently. In this corner of the phase space this mechanism may be more effective than gluon fusion because the later generates final mesons with a x_F distribution peaked at zero. This possibility was explored in [23].

The appearance of the first LHCb data on asymmetries [8] opens the exciting possibility of studying the energy dependence of forward charm production. Indeed, more than ten years from the last data on this subject, we have now data taken at an energy which is larger than the previous one by a factor of $\simeq 200$! What do the models discussed above have to say about the energy dependence of forward charm production? What will be the fate of the production asymmetries ? The answer to this question is interesting not only to the hadron physics community but also to the studies of CP violation, since a change in the relative yield of particles and antiparticles may affect the interpretation of their decays and hence change the ammount of CP violation.

Naively, we expect that perturbative processes grow faster and become more important than non-perturbative ones as the reaction energy increases. As a consequence the asymmetries would gradually disappear. In [24] a kinematical treatment of this problem arrived at the conclusion that, as the energy grows, the energy deposition in the central region increases, baryon stopping also increases and the remnant valence quarks emerge from the collision with less energy. Even though the sources of asymmetry would still be operating, because of the increasing stopping of the valence quarks, the outgoing charm mesons with these quarks would be decelerated and their x_F distribution would become invisible, buried under the much higher contribution from the (symmetric) central gluon fusion. In [16], using a recombination approach, the authors concluded that the asymmetry remains nearly constant with energy. In the meson cloud approach of [22] the energy dependence of the asymmetry A is approximately given by:

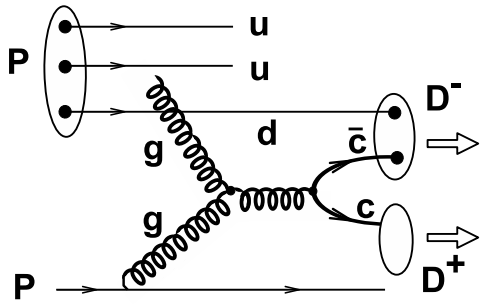

FIG. 1: D meson production in a proton - proton reaction. The charm pair is created by gluon fusion and then the quarks may fragment independently, as it happens to the c quark in figure, or they can "recombine" or "coalesce" with one of the projectile valence quarks, as it is the case of the $\bar{c}$ in the figure. Mesons formed by recombination are harder since they are "dragged" by the hard valence quark.

$$A \propto \frac{\sigma_{hp}(s)}{\sigma_{c\bar{c}}(s)} \tag{2}$$

where σ_{hp} is hadron-proton cross section and $\sigma_{c\bar{c}}$ is the total $c\bar{c}$ pair production cross section, which grows faster than the hadronic cross sections. Therefore the asymmetry decreases with the energy.

In this work we use the model developed in [22] to study the recent LHCb data on D^+/D^- asymmetry and to check if the energy behavior of this asymmetry can be satisfactorily understood with this model. The paper is organized as follows. In the next Section, we discuss the asymmetry production in terms of the meson cloud model, presenting the main formulas and assumptions of the model. In Section III we present our results for the asymmetries in Λ and D production at SELEX ($\sqrt{s} = 33$ GeV) and LHCb ($\sqrt{s} = 7$ TeV) energies. We compare the results with the current data and make predictions for $\sqrt{s} = 14$ TeV. Finally, in Section IV we summaryze our main conclusions.

II. ASYMMETRY PRODUCTION IN THE MESON CLOUD MODEL

A. The interaction between the cloud and the target

In the MCM we assume that quantum fluctuations in the projectile play an important role. The proton may be decomposed in a series of Fock states, containing states

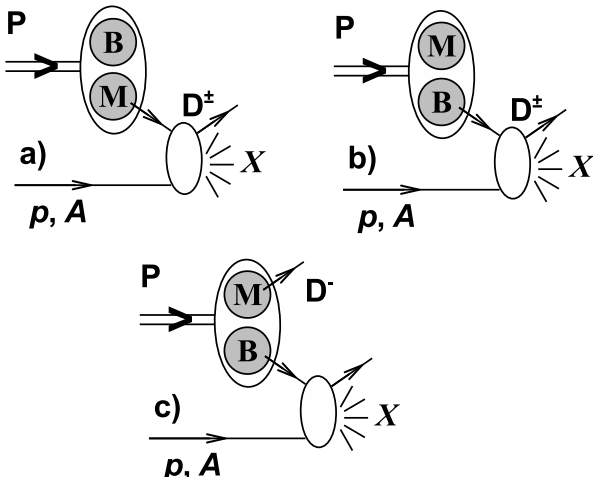

FIG. 2: pp collision in which the projectile is in a $|MB\rangle$ state. Figs. a) and b) show the "indirect" $D^{\pm}$ production and c) the "direct" D^- production.

such as $|p\rangle = |uud\bar{c}c\rangle$. In the MCM we write the Fock decomposition in terms of the equivalent hadronic states, such as $|p\rangle = |\Sigma_c^{++} D^-\rangle$. This expansion contains the "bare" terms (without cloud fluctuations), light states and states containing the produced charmed meson (D or D_s). The latter are, of course very much suppressed but they will be responsible for asymmetries. The "bare" states occur with a higher probability and are responsible for the bulk of charm meson production at low and medium momentum ($x_F \leq 0.4$), including, for example the perturbative QCD contribution. The cloud states are less frequent fluctuations and contribute to D production in the ways described below. More precisely we shall assume that:

$$|p\rangle = Z\,[\,|p_0\rangle + ... + |MB\rangle + ... + |\Lambda_c \bar{D}_0\rangle + |\Sigma_c^{++} D^-\rangle] \quad (3)$$

where Z is a normalization constant, $|p_0\rangle$ is the "bare" proton and the "dots" denote all possible meson (M) - baryon (B) cloud states $|MB\rangle$ in the proton. The relative normalization of these states is fixed once the cloud parameters are fixed. The proton is thus regarded as being a sum of virtual meson-baryon pairs and a proton-proton reaction can thus be viewed as a reaction between the "constituent" mesons and baryons of the projectile proton with the target proton (or nucleus).

With a proton beam the possible reaction mechanisms for D^- meson production at large x_F and small p_T (the soft regime) are illustrated in Fig. 2. In Fig. 2 a) the baryon just "flies through", whereas the corresponding meson interacts inelastically producing a D meson in the final state. In Fig. 2 b) the meson just "flies through", whereas the corresponding baryon interacts inelastically producing a D meson in the final state. In Fig. 2 c) the meson in the cloud *is already a* D^- which escapes (similar considerations hold for D^- production with a π^- beam). This last mechanism is the main responsible for generating asymmetries. We shall refer to the first two processes as "indirect production" (I) and to the last one as "direct production" (D). The first two are calculated with convolution formulas whereas the last one is given basically by the meson momentum distribution in the initial $|MB\rangle$ cloud state. Direct production has been widely used in the context of the MCM and applied to study n, Δ^{++} and π^0 production [19]. Indirect meson production has been considered previously in [20].

Inside the baryon, in the $|MB\rangle$ state, the meson and baryon have fractional momentum y_M and y_B with distributions called $f_{M/MB}(y_M)$ and $f_{B/MB}(y_B)$ respectively (we shall use for them the short notation f_M and f_B). Of course, by momentum conservation, $y_M + y_B = 1$ and these distributions are related by [18, 20]:

$$f_M(y) = f_B(1-y) \quad (4)$$

The "splitting function" $f_M(y)$ represents the probability density to find a meson with momentum fraction y of the total cloud state $|MB\rangle$. With f_M and f_B we can compute the differential cross section for production of D, $\bar{D}_0$ and Λ_c. In what follows we write the formulas for the specific case of D production but it is easy, with the proper replacements, to write the corresponding expressions for $\bar{D}_0$ and Λ_c. In the reaction $pp \to D^- X$ the differential cross section for D production is given by:

$$\frac{d\sigma^{pp\to DX}}{dx_F} = \Phi_0 \; + \; \Phi_I \; + \; \Phi_D \quad (5)$$

where Φ_0 and Φ_I refer respectively to "bare" and indirect contributions to D meson production and x_F is the fractional longitudinal momentum of the outgoing meson. Φ_D represents the direct process depicted in Fig. 2 c) and is given by [19, 20]:

$$\Phi_D = \frac{\pi}{x_F}\, f_D(x_F)\, \sigma^{\Sigma p} \quad (6)$$

where $f_D \equiv f_{D^-/\Sigma_c^{++} D^-}$ and $\sigma^{\Sigma p}$ is the total $p\,\Sigma_c^{++}$ cross section. Replacing $D^{\pm}$ by $\Lambda_c/\bar{\Lambda}_c$ in Figs. 2a and 2b, exchanging B with M and replacing D^- by Λ_c in Fig. 2 c) we have a pictorial representation of Λ_c production in the MCM with the following expression for the direct process:

$$\Phi_D = \frac{\pi}{x_F}\, f_\Lambda(x_F)\, \sigma^{Dp} \quad (7)$$

where $f_\Lambda \equiv f_{\Lambda_c/\Lambda_c \bar{D}_0}$ and σ^{Dp} is the total $\bar{D}_0\, p$ cross section. Analogous expressions can be written for the reaction $\pi^- p \to DX$.

B. The asymmetry

Using (5), we can compute the cross sections and also the leading (D^-)/nonleading(D^+) asymmetry:

$$\begin{aligned} A^D(x_F) &= \frac{\frac{d\sigma^{D^-}(x_F)}{dx_F} - \frac{d\sigma^{D^+}(x_F)}{dx_F}}{\frac{d\sigma^{D^-}(x_F)}{dx_F} + \frac{d\sigma^{D^+}(x_F)}{dx_F}} \\ &= \frac{\Phi_D + \Phi_I^{D^-} + \Phi_0^{D^-} - \Phi_I^{D^+} - \Phi_0^{D^+}}{\Phi_D + \Phi_I^{D^-} + \Phi_0^{D^-} + \Phi_I^{D^+} + \Phi_0^{D^+}} \\ &\simeq \frac{\Phi_D}{\Phi_D + 2\,\Phi_I^D + 2\,\Phi_0^D} \equiv \frac{\Phi_D}{\Phi_T^D} \end{aligned} \tag{8}$$

where the last line follows from assuming $\Phi_I^{D^-} = \Phi_I^{D^+} = \Phi_I^D$. This last assumption is made just for the sake of simplicity. In reality these contributions are not equal and their difference is an additional source of asymmetry, which we assume to be less important than Φ_D. Since the "bare" states do not give origin to D^-/D^+ asymmetries (they represent mostly perturbative QCD contributions which rarely leave quark pairs in the large x_F region), we have made use of $\Phi_0^{D+} = \Phi_0^{D-} = \Phi_0^D$. The denominator of the above expression can be replaced by a parametrization of the experimental data:

$$\begin{aligned} \Phi_T^D &= \frac{d\sigma^{D^-}(x_F)}{dx_F} + \frac{d\sigma^{D^+}(x_F)}{dx_F} \\ &= \sigma_0^D\,[\,(1-x_F)^{n^-} + (1-x_F)^{n^+}\,] \\ &\simeq 2\,\sigma_0^D\,(1-x_F)^{n_D} \end{aligned} \tag{9}$$

where n^- and n^+ are powers used by the different collaborations to fit their data. Typically $n^+ = 5$ and $n^- = 3.5$, as suggested by the data analysis performed in [1–6]. For the sake of simplicity we shall assume that $n^+ = n^- = n_D = 5$ for D mesons. Integrating the above expression we obtain the total cross section for charged charm meson production $\sigma^{D^\pm} = 1/3\,\sigma_0^D$. Assuming isospin symmetry the charged and neutral (σ^{D^0}) production cross sections are equal. Neglecting the contribution of other (heavier) charm states we can relate the D meson production cross section to the total $c-\bar{c}$ production cross section, $\sigma_{c\bar{c}}$, in the following way:

$$\sigma^{D^\pm} = \sigma^{D^0} = \sigma^D = \frac{1}{3}\sigma_0^D = \frac{1}{2}\sigma_{c\bar{c}}\ . \tag{10}$$

From the above relation we can extract the parameter σ_0^D from the experimentally measured $\sigma_{c\bar{c}}$:

$$\sigma_0^D = 1.5\,\sigma_{c\bar{c}}\ . \tag{11}$$

Inserting (6) and (9) into (8) the asymmetry becomes:

$$A^D(x_F) = \frac{\pi\,\sigma^{\Sigma p}}{2\,\sigma_0^D}\ \frac{f_D(x_F)}{x_F\,(1-x_F)^{n_D}}\ . \tag{12}$$

An analogous development can be performed for the $\Lambda_c/\bar{\Lambda}_c$ production asymmetry, $A^\Lambda(x_F)$. In the analysis made by the SELEX collaboration, the differential cross section for Λ_c production was parametrized as:

$$\begin{aligned} \Phi_T^\Lambda &= \frac{d\sigma^{\Lambda_c}(x_F)}{dx_F} + \frac{d\sigma^{\bar{\Lambda}_c}(x_F)}{dx_F} \\ &\simeq 2\,\sigma_0^\Lambda\,(1-x_F)^{n_\Lambda} \end{aligned} \tag{13}$$

with $n_\Lambda \simeq 2$. Integrating the above expression we obtain the total cross section for Λ_c and $\bar{\Lambda}_c$ production $\sigma^\Lambda = 2/3\,\sigma_0^\Lambda$, which, according to [25], can be related to the total $c-\bar{c}$ production cross section, $\sigma_{c\bar{c}}$, in the following way:

$$\sigma^\Lambda = \frac{2}{3}\sigma_0^\Lambda \simeq 0.1\,\sigma_{c\bar{c}} \tag{14}$$

from where we finally have:

$$\sigma_0^\Lambda = 0.15\,\sigma_{c\bar{c}}\ . \tag{15}$$

Using (4) to obtain f_Λ and then inserting (7) and (13) into (8) the asymmetry $A^\Lambda(x_F)$ can be written as:

$$A^\Lambda(x_F) = \frac{\pi\,\sigma^{Dp}}{2\,\sigma_0^\Lambda}\ \frac{f_\Lambda(x_F)}{x_F\,(1-x_F)^{n_\Lambda}} \tag{16}$$

The behavior of (12) [Eq. (16)] is controlled by the splitting function $f_D(x_F)$ [$f_\Lambda(x_F)$].

C. The splitting function

We now write the splitting function in the Sullivan approach [18, 20]. The fractional momentum distribution of a pseudoscalar meson M in the state $|MB'\rangle$ (of a baryon $|B\rangle$) is given by [18, 20]:

$$\begin{aligned} f_M(y) &= \frac{g^2_{MBB'}}{16\pi^2}\,y\int_{-\infty}^{t_{max}} dt\,\frac{[-t+(m_{B'}-m_B)^2]}{[t-m_M^2]^2} \\ &\times\ F^2_{MBB'}(t) \end{aligned} \tag{17}$$

where t and m_M are the four momentum square and the mass of the meson in the cloud state and $t_{max} = m_B^2\,y - m_{B'}^2\,y/(1-y)$ is the maximum t, with m_B and $m_{B'}$ respectively the B and B' masses. Following a phenomenological approach, we use for the baryon-meson-baryon form factor $F_{MBB'}$, the exponential form:

$$F_{MBB'}(t) = \exp\left(\frac{t-m_M^2}{\Lambda^2_{MBB'}}\right) \tag{18}$$

where $\Lambda_{MBB'}$ is the form factor cut-off parameter.

Considering the particular case where $B = p$, $B' = \Sigma_c^{++}$ and $M = D^-$, we insert (17) into (12) to obtain the final expression for the asymmetry in our approach:

$$\begin{aligned} A^D(x_F) &= \frac{N^D}{(1-x_F)^{n_D}} \\ &\times\ \int_{-\infty}^{t_{max}} dt\,\frac{[-t+(m_\Sigma-m_p)^2]}{[t-m_D^2]^2}\,F^2_{pD\Sigma} \end{aligned} \tag{19}$$

where

$$N^D = \frac{g^2_{pD\Sigma_c}\,\sigma^{\Sigma_c p}}{32\,\pi\,\sigma_0^D} \tag{20}$$

With the replacements $g_{pD\Sigma_c} \to g_{pD\Lambda_c}$ and $\sigma^{\Sigma_c p} \to \sigma^{\Lambda_c p}$ this same expression holds for the process $pp \to \bar{D}_0 X$. With the replacements $g_{pD\Sigma_c} \to g_{pD\Lambda_c}$, $\sigma^{\Sigma_c p} \to \sigma^{Dp}$ and $\sigma_0^D \to \sigma_0^\Lambda$ the above expression holds for the process $pp \to \Lambda_c X$. For the pion beam, we need also the splitting function of the state $|\pi^- > \to |D^{0*} D^-\rangle$. In this state, the D meson momentum distribution turns out to be identical to (17) except for the bracket in the numerator which takes the form $[-t + \left((m_\pi^2 - m_{D^{0*}}^2 - t)/2m_{D^{0*}}\right)^2]$, and for trivial changes in the definitions, i.e., $g^2_{MBB'} \to g^2_{\pi DD^{0*}}$, $F_{MBB'} \to F_{\pi DD^{0*}}$ and $\Lambda_{MBB'} \to \Lambda_{\pi DD^{0*}}$. Realizing that $y = x_F$ in the above equations, we can see that in the limit $x_F \to 1$, $t_{max} \to -\infty$ and the integral in (19) goes to zero. In fact, it vanishes faster than the denominator and therefore $A \to 0$. This behavior does not depend on the cut-off parameter but it depends on the choice of the form factor. For a monopole form factor we may obtain asymmetries which grow even at very large x_F.

We emphasize that i.) our calculation is based on quite general and well established ideas, namely that hadron projectiles fluctuate into hadron-hadron (cloud) states and that these states interact with the target; ii.) our results depend only on two parameters: Λ and N. Whereas Λ affects the width and position of the maximum of the momentum distribution of the leading meson in the cloud (and consequently of the asymmetry), N is a multiplicative factor which determines the strength of the asymmetry.

III. RESULTS AND DISCUSSION

A. The energy dependence

Although the recent data [8] are given in terms of the pseudo-rapidity η, in order to study the energy dependence it is more convenient to use the Feynman x_F variable, which may be written as:

$$x_F = \frac{2\,m_T\,cosh(y)}{\sqrt{s}} \simeq \frac{2\,m_T\,cosh(\eta)}{\sqrt{s}} \simeq \frac{2\,m_T\,e^\eta}{\sqrt{s}}$$

for $\eta > 1$. Moreover, if the transverse momentum of the final D meson is zero or very small, then $m_T \simeq m_D$.

In order to study the energy dependence of the asymmetry, we shall focus on the two energies where we have experimental data: $\sqrt{s_1} = 33$ GeV and $\sqrt{s_2} = 7000$ GeV and construct the asymmetry ratio:

$$R_A \equiv \frac{A(\sqrt{s_2})}{A(\sqrt{s_1})} = \frac{\Phi_D(\sqrt{s_2})/\Phi_T(\sqrt{s_2})}{\Phi_D(\sqrt{s_1})/\Phi_T(\sqrt{s_1})}\ . \tag{21}$$

Energy (GeV)	σ_{pp} (mb)	$\sigma_{c\bar{c}}$ (mb)
33	40	0.04
7000	97	8
14000	110	11

TABLE I: Total pp cross section from [26] and total $c\bar{c}$ production cross section from [27] as a function of the energy. The first two lines refer to measurements and the last one show model calculations described in the corresponding references.

Using the definitions of the splitting function (17) in (6) and then in (8), many energy independent factors cancel out and we find:

$$\begin{aligned} R_A &= \frac{A(s_2)}{A(s_1)} = \left(\frac{\sigma^\Sigma(s_2)}{\sigma^\Sigma(s_1)}\right) / \left(\frac{\sigma_0^D(s_2)}{\sigma_0^D(s_1)}\right) \\ &= \left(\frac{\sigma^{pp}(s_2)}{\sigma^{pp}(s_1)}\right) / \left(\frac{\sigma_{c\bar{c}}(s_2)}{\sigma_{c\bar{c}}(s_1)}\right) \end{aligned} \tag{22}$$

where in the last step we have used (11) and assumed that $\sigma^\Sigma = \sigma^{\Sigma_c^{++}\,p} = \text{const}\,.\,\sigma^{p\,p}$. Moreover, we have neglected the energy dependence of n_D. The above ratios can be estimated with the recently obtained experimental data listed in Table I.

With these numbers we find that increasing the energy the asymmetry ratio is $R_A = 1/75$, i.e., there is a strong decrease in the asymmetry. This happens because the responsible for the asymmetry is meson emission, a non-perturbative process, which has a slowly growing cross section. In contrast, the symmetric processes are driven by the perturbative partonic interactions, which have strongly growing cross sections. We end this subsection making the prediction for the order of magnitude of the D^+/D^- asymmetry in the forthcoming 14 TeV pp collisions. Using the last line of Table I, setting $\sqrt{s_2} = 14$ TeV and susbtituting the numbers in (22) we find $R_A = 1/100$ showing the decreasing trend of the asymmetry.

B. Predictions for the asymmetries

Due to the lack of experimental data a direct comparison of D^+/D^- asymmetries in the same reaction, e.g. proton-proton, at different energies is difficult. However, we can relate and compare similar reactions. In what follows we shall relate the two sets of data on asymmetries in proton-proton collisions: the low energy one taken by the SELEX collaboration [6] and the high energy one obtained by the LHCb collaboration [8]. We will fit the data on $\Lambda_c/\bar{\Lambda}_c$ asymmetry. This will fix the value of N^Λ and define a range of possible values for the cut off $\Lambda_{\bar{D}_0 p\Lambda_c}$. Using experimental information it is easy to go from the estimate of N^Λ to the estimate of N^D and then it is straightforward to calculate the associate asymmetry

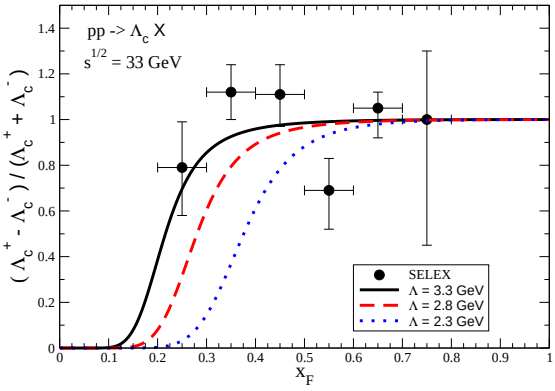

FIG. 3: Comparison of the MCM asymmetry for Λ_c production with experimental data [6] for $\sqrt{s} = 33$ GeV.

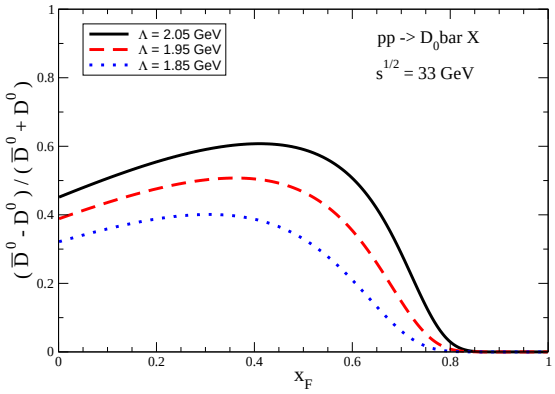

FIG. 4: MCM prediction of the $\bar{D}^0/D^0$ asymmetry, Eq. (19).

in $\bar{D}_0/D_0$. In proton-proton collisions the leading charm mesons are those with valence quarks and hence $\bar{D}_0(u\bar{c})$ has the same properties as $D^-(d\bar{c})$. From this approximate equivalence we infer the D^-/D^+ asymmetry at the lower energy. The final step is to calculate this asymmetry at the LHC energy. This extrapolation can be done, since the model has a well defined energy dependence and fortunately the necessary ingredients (the cross sections) are already available.

1. *The coupling constants*

The coupling constant $g_{pD\Lambda_c}$ was estimated in several works with QCD sum rules [28]. Here we have chosen a representative number. In our analysis we will also need the coupling $g_{pD^-\Sigma_c^{++}}$, about which, to the best of our knowledge, nothing is known. As a first guess we will then assume that

$$g_{pD^-\Sigma_c^{++}} = g_{p\bar{D}_0\Lambda_c} = 5.6 \ . \tag{23}$$

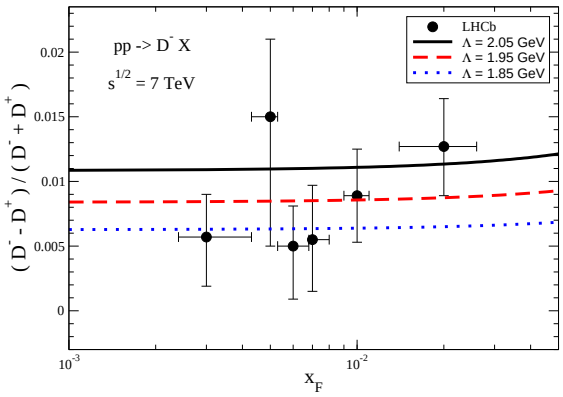

FIG. 5: Comparison of the MCM asymmetry, Eq. (19), with experiental data [8] for D^-/D^+.

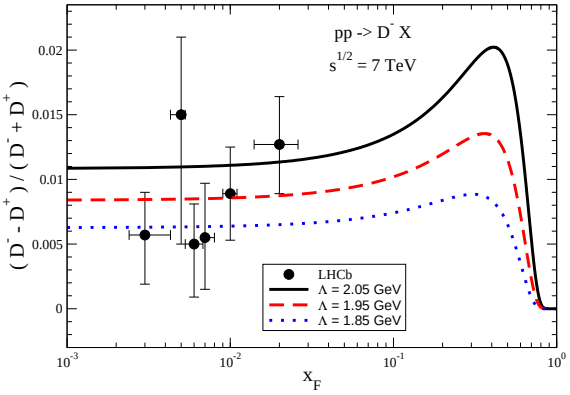

FIG. 6: Comparison of the MCM asymmetry, Eq. (19), with experimental data [8] for D^-/D^+. Extension of Fig. 5 to the large x_F region.

2. *The interaction cross sections of the cloud particles*

The D - proton and Λ_c - proton total cross sections in the $10-40$ GeV range are unknown. We might know them better in the future from the CBM and PANDA experiments at FAIR. We know that the presence of the heavy quark makes these states much more compact than the proton and hence with smaller geometrical cross section. In the well studied case of the J/ψ - proton cross section, a series of theoretical works gradually converged to $\sigma^{J/\psi p} \simeq 4$ mb [29]. Moreover, it was found that, in contrast to the expectation of additive quark models, $\sigma^{J/\psi p} \simeq \sigma^{J/\psi \pi}$. Inspired by these previous works we shall assume that:

$$\sigma^{Dp} \simeq \sigma^{\Lambda_c p} = 0.15\, \sigma^{pp} = 6\,\text{mb} \ . \tag{24}$$

$g_{pD\Lambda_c}$	σ^{Dp}	σ_0^{Λ}	$\sigma^{\Lambda_c p}$	σ_0^{D}
5.6	0.15 σ^{pp}	0.15 $\sigma_{c\bar{c}}$	0.15 σ^{pp}	1.5 $\sigma_{c\bar{c}}$

TABLE II: Parameters used to calculate N at $\sqrt{s} = 33$ GeV.

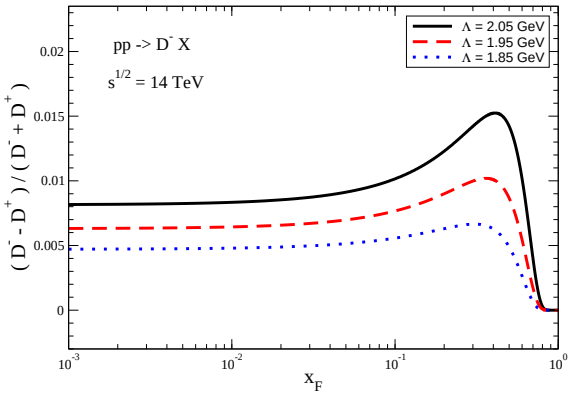

FIG. 7: Prediction of the D^-/D^+ asymmetry for $\sqrt{s} = 14$ TeV.

3. *The production cross sections of the charm particles*

The production cross section of charmed hadrons is measured in some cases and calculated with pQCD in others. In order to have an estimate of these cross sections it is enough for our present purposes to use the pQCD results published in [25], from where we have deduced (11) and (15). All this information is summarized in Table II. Starting from the definition (20) and using the numbers given in Table II we have:

$$N^{\Lambda} = \frac{g^2_{pD\Lambda_c}}{32\,\pi}\frac{\sigma^{Dp}}{\sigma_0^{\Lambda}} = \frac{(5.6)^2}{32\,\pi}\frac{0.15\,\sigma^{pp}}{0.15\,\sigma_{c\bar{c}}} \simeq 320 \qquad (25)$$

and also:

$$N^{D} = \frac{g^2_{pD\Lambda_c}}{32\,\pi}\frac{\sigma^{\Lambda_c p}}{\sigma_0^{D}} = \frac{(5.6)^2}{32\,\pi}\frac{0.15\,\sigma^{pp}}{1.5\,\sigma_{c\bar{c}}} \simeq 32 \qquad (26)$$

In Fig. 3, we show the $\Lambda_c/\bar{\Lambda}_c$ asymmetry in pp collisions at $\sqrt{s} = 33$ GeV. The experimental points are the results obtained by the SELEX collaboration. The lines are calculated with Eq. (16) with the normalization fixed by (25). These data can not impose a stringent contraint on the model, but they can establish a range of acceptable values for the cut-off parameter, which values are shown in the figure. The outcoming numbers for Λ are those expected in this kind of meson cloud calculation. If they had been smaller than 1 GeV or larger than 5, this would have been an evidence against the model.

In Fig. 4, we show the $\bar{D}_0/D_0$ asymmetry in pp collisions at $\sqrt{s} = 33$ GeV. It was calculated with Eq. (19) with the normalization factor given by (26). Since N^D is fixed the only free parameter is the cut-off Λ, which, as it will be seen next, will be fixed so as to yield a good fit

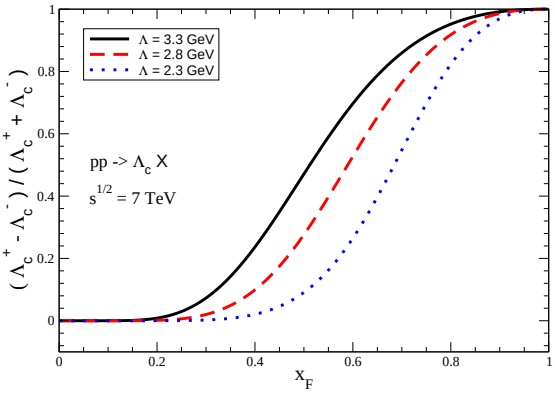

FIG. 8: Prediction of the $\Lambda_c/\bar{\Lambda}_c$ asymmetry for $\sqrt{s} = 7$ TeV.

of the D^+/D^- asymmetry data from the LHCb collaboration. Also in this case, the values of Λ used to draw the curves are quite reasonable. The shapes of Figs. 3 and 4 are correlated since they refer to the same vertex, where the proton splitts into a meson $\bar{D}_0$ and a baryon Λ_c. Due to its larger mass the baryon takes most of the momentum and the resulting asymmetry peaks at very large values of x_F. Complementarily, the $\bar{D}_0$ distribution peaks at lower values of x_F, which, nevertheless, are still large. The value of the cut-off Λ does not have to be the same as that used in Fig. 3 because, even though the coupling constant of a given vertex is always the same, the functional form of the form factor (as a function of the off-shell particle squared momentum) changes when the off-shell particle changes.

Neglecting differences coming from the different isospin, we assume that, apart from trivial changes in the masses, the vertex $p\Sigma_c^{++}D^-$ has the same splitting function as the previously discussed $p\Lambda_c\bar{D}_0$ vertex and therefore the asymmetry of D^- production is given by the same expression used for the $\bar{D}_0$. Now we try to reproduce the $\sqrt{s} = 7$ TeV LHCb data with Eq. (19). The only part of this expression which depends on the energy is the factor N^D, which at higher energies will be corrected by the factor (22):

$$\begin{aligned} N^D(\sqrt{s} = 7\,\text{TeV}) &= R_A\,.\,N^D(\sqrt{s} = 33\,\text{GeV}) \\ &= \frac{1}{75}\,N^D(\sqrt{s} = 33\,\text{GeV}) \end{aligned} \qquad (27)$$

In Fig. 5 we show Eq. (19) with $N^D(\sqrt{s} = 7\,\text{TeV})$ and compare with the data, properly rewritten in terms of x_F and with the definition (8), which introduces a minus sign with respect to [8]. In spite of the large error bars we can see that the MCM is able to reproduce the non-vanishing asymmetry. The data are surprisingly sensitive to cut-off choices, being able to discriminate small variations in Λ. These data can not yet give a detailed information about the x_F dependence of the asymmetry, but they show clearly that this asymmetry exists and also that it is much smaller than what we expect to find at lower energies for pp and than what we have already found for pion and Σ projectiles. After this close look into the data

points, this figure deserves a zoom out to reach the x_F region which was scanned in previous lower energies experiments. This is shown in Fig. 6, from where we draw the most important conclusion of this work: the asymmetry definitely decreases at increasing energies, reaching at most 2 % at $x_F \simeq 0.4$. Finally, in Fig. 7 we show our prediction for the asymmetry to be measured at $\sqrt{s} = 14$ TeV. For completeness, we present in Fig. 8 our predictions for the Λ_c asymmetry at $\sqrt{s} = 7$ TeV.

IV. SUMMARY

In this paper we have shown that the MCM provides a good understanding of the charm production asymmetries in terms of a simple physical picture with few parameters. It connects the behavior of the asymmetries at large x_F with the charm meson momentum distribution within the cloud state. We can explain why we observe asymmetries, why they are different for different beams and why they decrease with increasing energies.

Acknowledgments

This work has been partially supported by CNPq and FAPESP.

[1] M. I. Adamovich *et al.*, (WA82 Collab.), Phys. Lett. B **306**, 402 (1993).

[2] G. A. Alves *et al.*, (E769 Collab.), Phys. Rev. Lett. **77**, 2392 (1996).

[3] E. M. Aitala *et al.*, (E791 Collab.), Phys. Lett. B **411**, 230 (1997).

[4] M. I. Adamovich *et al.*, (WA92 Collab.), Nucl. Phys. B **495**, 3 (1997).

[5] M. I. Adamovich *et al.*, (WA89 Collab.), Eur. Phys. J. C **8**, 593 (1999); C **13**, 247 (2000).

[6] F.G. Garcia *et al.* (SELEX Collab.) Phys. Lett. B **528**, 49 (2002); M. Iori *et al.*, (SELEX Collab.), Nucl. Phys. B (Proc. Suppl.) **75** , 16 (1999); hep-ex/0009049; J.C. Anjos and E. Cuautle, hep-ph/0005057.

[7] C. Adolph *et al.* [COMPASS Collaboration], arXiv:1211.1575 [hep-ex].

[8] R. Aaij *et al.* [LHCb Collaboration], Phys. Lett. B. **718**, 902 (2013) [arXiv:1210.4112 [hep-ex]].

[9] F. S. Navarra, M. Nielsen, C. A. A. Nunes and M. Teixeira, Phys. Rev. D **54**, 842 (1996); S. Paiva, M. Nielsen, F. S. Navarra, F. O. Durães and L. L. Barz, Mod. Phys. Lett. A **13**, 2715 (1998); W. Melnitchouk and A.W. Thomas, Phys. Lett. B **414**, 134 (1997).

[10] S. J. Brodsky, P. Hoyer, C. Peterson and N. Sakai, Phys. Lett. B **93**, 451 (1980).

[11] R. Vogt, S. J. Brodsky and P. Hoyer, Nucl. Phys. B **360**, 67 (1991); R. Vogt and S. J. Brodsky, Nucl. Phys. B **438**, 261 (1995); Nucl. Phys. B **478**, 311 (1996); T. Gutierrez and R. Vogt, Nucl. Phys. **B539**, 189 (1999).

[12] K.P. Das *et al.*, Phys. Lett. B **68**, 459 (1977); Erratum-ibid. B **73**, 504 (1978); C.B. Chiu *et al.*, Phys. Rev. D **20**, 211 (1979).

[13] R. Hwa, Phys. Rev. D **22**, 1593 (1980); Phys. Rev. D **51**, 85 (1995).

[14] V.G. Kartvelishvili *et al.*, Sov. J. Nucl. Phys. **33**, 434 (1981); Yad. Fiz. **33**, 832 (1981); A.K. Likhoded *et al.*, Sov. J. Nucl. Phys. **38**, 433 (1983); Yad. Fiz. **38**, 727 (1983).

[15] E. Cuautle *et al.*, Eur. Phys. J. C **2**, 473 (1998); E. Braaten *et al.*, Phys. Rev. Lett. **89**, 122002 (2002); T. Mehen, Acta Phys. Polon. B **35**, 121 (2004); AIP Conf. Proc. **698**, 508 (2004); J. Phys. G **30**, S295 (2004); C. Avila, J. Magnin and L. M. Mendoza-Navas, hep-ph/0307358.

[16] R. Rapp and E. V. Shuryak, Phys. Rev. D **67**, 074036 (2003).

[17] A. D. Frawley, T. Ullrich and R. Vogt, Phys. Rept. **462**, 125 (2008)

[18] for a review see J. Speth and A. W. Thomas, Adv. Nucl. Phys. **24**, 83 (1998); S. Kumano, Phys. Rep. **303**, 183 (1998); A.W. Thomas, Phys. Lett. B **126**, 97 (1983).

[19] H. Holtmann, A. Szczurek and J. Speth, Nucl. Phys. A **569**,631 (1996); N. N. Nikolaev, W. Schaefer, A. Szczurek and J. Speth, Phys. Rev. D **60**, 014004 (1999).

[20] F. Carvalho, F. O. Durães, F. S. Navarra and M. Nielsen, Phys. Rev. D **60**, 094015 (1999); F. S. Navarra, M. Nielsen and S. Paiva, Phys. Rev. D **56**, 3041 (1997).

[21] M. Burkardt, K. S. Hendricks, C. -R. Ji, W. Melnitchouk and A. W. Thomas, arXiv:1211.5853 [hep-ph] and references therein.

[22] F. Carvalho, F. O. Duraes, F. S. Navarra and M. Nielsen, Phys. Rev. Lett. **86**, 5434 (2001).

[23] V. P. Goncalves, F. S. Navarra and T. Ullrich, Nucl. Phys. A **842**, 59 (2010).

[24] F. O. Durães, F. S. Navarra, C. A. A. Nunes and G. Wilk, Phys. Rev. D **53**, 6136 (1996).

[25] R. V. Gavai, S. Gupta, P. L. McGaughey, E. Quack, P. V. Ruuskanen, R. Vogt and X. -N. Wang, Int. J. Mod. Phys. A **10**, 2999 (1995).

[26] D. A. Fagundes, M. J. Menon and P. V. R. G. Silva, arXiv:1208.3456 [hep-ph].

[27] R. E. Nelson, R. Vogt and A. D. Frawley, Phys. Rev. C **87** 014908 (2013).

[28] F. S. Navarra and M. Nielsen, Phys. Lett. B **443**, 285 (1998); F. O. Duraes, F. S. Navarra and M. Nielsen, Phys. Lett. B **498**, 169 (2001) and references therein.

[29] H. G. Dosch, F. S. Navarra, M. Nielsen and M. Rueter, Phys. Lett. B **466**, 363 (1999); F. O. Duraes, S. H. Lee, F. S. Navarra and M. Nielsen, Phys. Lett. B **564**, 97 (2003).